Wiley
International Journal of Energy Research
Volume 2024, Article ID 5558323, 13 pages
https://doi.org/10.1155/2024/5558323

WILEY

Research Article

Syngas Purpose Pyrolysis-Gasification of Organic Fractions of MSW over Metal-Loaded Y-Zeolite Catalysts

Dominik Horváth,[1] **Szabina Tomasek**,[1] **Janka Bobek-Nagy**,[2] **Eliza Tóth**,[2] **Róbert Kurdi**,[2] **and Norbert Miskolczi**[1]

[1]*Faculty of Engineering, Research Centre of Biochemical, Environmental and Chemical Engineering, MOL Department of Hydrocarbon and Coal Processing, University of Pannonia, Egyetem u. 10, H-8200 Veszprém, Hungary*
[2]*Faculty of Engineering, Research Centre of Biochemical, Environmental and Chemical Engineering, Sustainability Solutions Research Lab, University of Pannonia, Egyetem u. 10, H-8200 Veszprém, Hungary*

Correspondence should be addressed to Szabina Tomasek; tomasek.szabina@mk.uni-pannon.hu

Received 22 October 2023; Revised 7 March 2024; Accepted 13 May 2024; Published 29 May 2024

Academic Editor: Maria Anna Murmura

The increasing environmental consideration and the growth of instability of the energy market call for methods that can process the organic fraction of municipal solid waste (OFMSW) into fuel instead of disposal. Due to the pyrolysis and gasification that are efficient procedures to achieve valuable products, gasification of OFMSW with different particle sizes and compositions was carried out in the presence of Ni and Ni-Ce-loaded Y-zeolite in a multizone tubular kiln reactor. During the experiments, 500°C was applied in the first reactor zone, while the 2nd zone was at an elevated temperature of 600°C or 900°C in the presence of steam. The combined pyrolysis and gasification experiments were also carried out without a catalyst with the same operating conditions. The feedstock was collected from the organic fraction of a Hungarian mechanical-biological treatment (MBT) plant and was separated into four different fractions based on particle size: <1 cm dry biomass and fine particles, 1-2 cm paper-rich, 2-6 cm paper and plastic-rich feedstocks, and <6 cm mixture of these fractions. During the experimental work, product yields; gaseous product composition; the ratio of H_2/CO, CO_2/CO, and CH_4/CO; and lower heating value were determined in the function of feedstock composition, the applied temperature, and catalysts. It was found that the hydrogen content and H_2/CO ratio of gaseous products were increased due to catalyst application and temperature elevation in the 2nd reactor zone. The addition of Ce to the Ni/Y-zeolite catalyst was advantageous in the case of hydrogen formation at a lower temperature (600°C). The hydrogen and methane content of products obtained from the catalytic pyrolysis-gasification of paper and plastic-rich OFMSWs on elevated temperatures were higher, which increased the lower heating value of those products. Based on the elemental analysis of the obtained solid residues, it was found that paper/plastic-rich feedstock released hydrogen and carbon with a higher extent. 1-2 cm feedstock-related solid residues had the highest H/C ratio which caused a 12.5-12.8 MJ/kg gross heating value. As a result, combined pyrolysis and gasification appear to be an efficient method to attain valuable outputs from OFMSW not only in gas but also in solid products.

1. Introduction

The increase in population and the improving life quality of societies have resulted in environmental challenges such as climate change and waste crisis. Although a slight decrease in energy demand could be observed during the global pandemic, at present, it has exceeded the prepandemic level by 1.8% [1]. Energy consumption is increasing year by year, while the unbalanced supply and demand and the current geopolitical situation led to severe price increases in the oil and gas market; therefore, need for alternative feedstock for energy production is greater than ever [2]. Municipal solid waste (MSW) generation is also growing globally, and it can reach 3.4 million tons by the year 2050 [3]. MSW accounts approximately 10% share of total waste generated in the European Union as well as based on the data reported.

Although the treatment of this waste is shifting towards reuse, material recycling, energy recovery, and chemical recycling, still, a significant amount of approximately 23% of MSW ends up in landfills [4]. Landfilling is a cheap and easy way, but even if the landfill structures are well engineered, it holds several environmental risks (e.g., water and soil pollution via leaching and air pollution via methane formation), i.e., landfilling is one of the worst strategies of waste management [5]. In the case when the collected MSW is processed in a mechanical-biological treatment (MBT) plant, which is the most usual process method of MSW in Europe, the organic fraction is mechanically sorted and defined as the undersized fraction of MSW (usually <50-80 mm) [6]. In most cases, the oversized fraction is processed further to energy use. The organic fraction of the MSW (OFMSW) is usually treated by biostabilization which means a 3-4 weeks long aerobic biological processing. However, as a result of aerobic stabilization, the weight is almost dimidiated, and the stabilized organic fraction is generally directed to the landfill [7]. Accordingly, that way of organic fraction treatment does not fit the circular economy approach and moreover does not comply with the EU Landfill Directive of April 1999 (99/31/EC) [8]. The Directive encourages the reduction of landfill of biodegradable compounds; moreover, it forces the decline of the total amount of deposited waste under 10% by 2035 (without derogation) [9]. The organic fraction of MSW can represent 40-85% of its mass. This, of course, depends on various factors, such as the economic situation of an area and the habits of the people living there [10]. Consequently, the reduction of the landfilled organic fraction is an essential step to fulfill the requirements of the Directive. Several techniques are available for OFMSW utilization [11]. Anaerobic digestion (AD) of OFMSW is an extensively researched method to enrich valuable end-products [12]. In addition to biogas production, the aim can be bioethanol, and biodiesel production, too [13]. The efficiency of AD can be improved by supplementing it with other processes such as hydrothermal carbonization to achieve biomethane and also high energy-density hydrochar [14]. Composting of OFMSW digestate is also a capable method to maximize the utilization of OFMSW [15]. In addition, pyrolysis and gasification of OFMSW are also promising methods [16] and result in the formation of valuable CO and H_2-rich syngas, liquid, and solid residue (char) [17]. The obtained syngas can be used as a feedstock for methanol or Fischer-Tropsch synthesis [18], while the liquid product can be used as an alternative hydrocarbon source for fuel and other high-value chemical production [19], i.e., pyrolysis and gasification can contribute to the reduction of landfilled waste providing a better waste treatment option [20] and alternative energy production at the same time [21]. Due to the abovementioned reasons, this treatment of MSW gained significant attention among researchers in the past years and several scientific papers and reviews have been made in the topic of pyrolysis and gasification [22]. Hasan et al. [23] provided a comprehensive review of the effect of process parameters (e.g., temperature, heating rate, residence time, and catalyst) and reactor type on the yield of pyrolysis products. Lu et al. [24] also summarized the effect of the operating parameters and reactor types of pyrolysis but examined the possibility of copyrolysis, too. In another paper [25], zeolite, dolomite, and oxide catalysts and their deactivation in MSW pyrolysis were investigated as well, and a technoeconomy analysis was also carried out. He et al. [26] also investigated the effects of dolomite catalyst. Their experiments were carried out in a bench-scale downstream fixed-bed reactor in a temperature range of 750-900°C. It was found that dolomite and higher reaction temperatures increased syngas production and resulted in a significant increase in H_2 and CO content. The beneficial effect was explained by cracking and reforming the high molecular weight organic components. The necessity of reforming reactions was also highlighted by Nandhini et al. [27]. ZSM-5 and Y zeolites are also widely used catalysts in syngas production. The more basic catalysts result in the formation of more CO, and strongly acidic catalysts are favorable for the production of hydrogen [28]. The strongly acidic ZSM-5 zeolite also has a positive effect for aromatic production and decreases the coke formation [29]. The catalyst arrangement also affects the processes taking place and the regenerability [30]. When the raw material and catalyst are previously mixed, the large molecules contact the catalyst more easily and react faster and the vapors diffuse into catalyst pores, where they undergo cracking and other reactions. However, the reusability of the used catalyst can be problematic. In contrast, when only pyrolysis vapors are in contact with the catalyst, the temperatures can be independently adjusted and catalyst separation and reuse do not cause problems either. Based on this fact, Wu and Williams [31] carried out pyrolysis-gasification experiments in a two-stage reactor system (raw material in the first zone, catalyst in the second zone). It is also well known that nickel impregnation of zeolites enhances hydrogen formation and reduces the amount of coke [32] as well as adding cerium as a promoter to the catalysts also increases syngas production [33]. The MSW composition is mainly determined by particle size; nonetheless, there is practically no publication about the effects of different particle sizes—consequently, different compositions—on yield, composition, and utilization of pyrolysis and gasification products, which significantly inhibits the rapid spread of chemical recycling of MSW.

Based on these facts, in this work, combined pyrolysis and gasification of OFMSW with different particle size was investigated in the presence of Ni/Y and Ni-Ce/Y-zeolite catalysts using a multizone tubular kiln reactor. Product yield, composition, and heating value were determined as functions of feedstock composition, temperature, and catalyst. Based on the results, critical evaluation was carried out in terms of utilization as well.

2. Material and Methods

2.1. Feedstock and Catalysts. MSW was originated from the biological fraction of a Hungarian MBT plant with 120 000 tonnes/year household solid waste capacity. The biological fraction is enriched from MSW after several mechanical processes. The first step of the mechanical processing is the

Table 1: Main components of feedstocks.

Component (%)	Feedstock			
	<1 cm; fine, soil-like	1-2 cm; paper rich	2-6 cm, paper and plastic rich	<6 cm mixed
Paper	—	54	38	24
Plastic	—	38	37	21
Textile	—	3	8	3
Other organic and fines	84	3	11	49
Hazardous (e.g., medical waste)	—	2	6	3
Small particle-sized visible extraneous material (e.g., plastic and glass)	16	N/D	N/D	N/D

Table 2: Main properties of different MSW feedstocks.

	Feedstocks			
	<1 cm; fines	1-2 cm; paper rich	2-6 cm; paper and plastic rich	<6 cm; mixed
Elemental analysis				
C (%)	19.7	34.6	41.6	35.6
H (%)	2.6	4.6	5.6	4.7
N (%)	1.2	1.3	1.3	1.8
S (%)	—	0.2	0.2	—
O (%)	20.3	13.5	27.5	23.2
O + other elements (e.g., Si, Ca, Al, Fe, K, Cl, and P) (%)	76.5	59.3	51.3	57.9
Proximate analysis				
Moisture (%)	6.8	6.5	5.0	7.7
Volatile (%)	25.3	40.2	59.9	51.4
Fixed carbon (%)	11.8	7.4	4.7	12.7
Ash* (%)	56.2	45.8	30.4	28.1

*In the determination of ash content, it was assumed that the residue obtained from thermogravimetric analysis consists of inert materials from the perspective of the pyrolysis, such as CaO, Al_2O_3, SiO_2, and MgO.

weighting and shredding of the waste into 250-350 mm particle size. Afterward, the magnetizable metals are separated. The next step is a rotary sieve wherein the biological waste stream under 80 mm particle size is removed for further treatment, which means a biological stabilization process. After all, the stable biological fraction is deposited into the landfill. The residue over 80 mm is driven to further separation processes to remove the aluminum and heavy fractions (stones, glass) and to achieve the plastic-rich RDF (refuse-derived fuel) fraction.

The laboratory samples were originated from the raw biological fraction directly after the rotary sieve separation step. The batch of the biological fraction was stabilized at the laboratory of the waste management team for 28 days in the air. The sample was divided into portions according to the rule of solid sample division. One part of the stabilized biological sample was sieved through 1, 2, and 6 cm size sieves to earn the different particle size fractions. The other part of the sample was a bulk fraction (particle size less than 6 cm) of the batch. The composition of the four different particle size fractions was determined by manual sorting. The fraction under 1 cm contained mainly biodegradable material (84%) like woody biomass, animal bones, and fine, soil-like components with 16% of "extraneous material" (stones, glass, plastic, etc.). 1-2 cm particle-sized fraction contained mainly paper, while the 2-6 cm feedstock had two main components: plastic (37%) and paper (38%). The main part of bulk feedstock (<6 cm) was organic material. Table 1 shows the composition of each feedstock. After the separation, the fractions were ground in order to increase the homogeneity and maintain the constant feed composition. It is important to note that metal, stones, and glass were removed from feedstocks, due to their chemically inert nature at the condition of pyrolysis and gasification. The results of the elemental analysis are summarized in Table 2. As data shows, 2-6 cm feedstock had the highest carbon and hydrogen content, while the <1 cm material was rich in oxygen and other elements like Si, Ca, Al, Fe, K, Cl, and P. Paper and plastic contributed to the C and H content of the feedstock while the high rate of O + other elements was provided by the biomass and fine content (Table 2).

The Ni/Y-zeolite and Ni-Ce/Y-zeolite were prepared by wet impregnation of commercial Y-zeolite (Alfa Aesar; surface area: 780 m^2/g; SiO_2/Al_2O_3 (molar): 80). At first, 1 M solution of $Ni(NO_3)_2 \bullet 6H_2O$ was mixed and stirred with zeolite for 2 hours at 80°C. After, the solid was filtered, dried (10 h, 110°C), and calcined for 3 h at 600°C. One part of the Ni/Y-zeolite was also impregnated with 0.02 M $(NH_4)_2Ce(NO_3)_6$ solution. Further steps were the same as

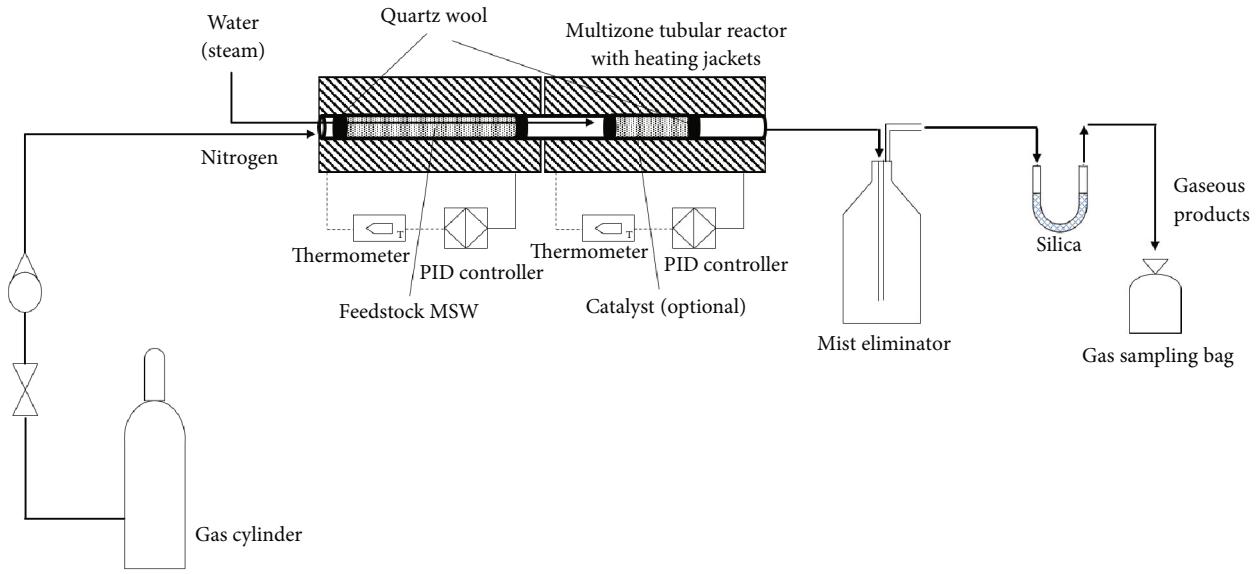

Figure 1: The scheme of the experimental apparatus.

the previous preparation process. The thus prepared Ni/Y-Zeolite contained 6.1% Ni while Ni-Ce/Y-zeolite contained 5.8% Ni and 0.9% Ce.

2.2. Combined Pyrolysis and Gasification Process and Experimental Apparatus. The thermal and thermocatalytic experiments were carried out in a multizone tubular kiln reactor (Figure 1). The reactor employed for the experiments is a furnace with a tube-in-tube configuration, equipped with separately heatable zones. The electric heating is provided by heating coils, which heat up a ceramic tube. The feedstock and the catalyst can be placed in separate tubes, with a diameter smaller than the ceramic tube. The furnace has a horizontal arrangement, and throughout the entire length of the tube, the gases produced during pyrolysis-gasification are present. The closing element of the reactor allows the introduction of gases, such as inert nitrogen, which prevents the combustion of the feedstock, and ensures the expulsion of the obtained gas products from the apparatus. Any potentially condensable components can condense in a mist eliminator. During the experiments, 5.0 g of OFMSW feedstock was used in the first reactor zone at 500°C. In the case of thermocatalytic pyrolysis-gasification, 2.5 g of catalyst was applied in the second (catalytic) zone at a temperature of 600 or 900°C. The same temperatures were applied in the second reaction zone during thermal pyrolysis-gasification as well. The heating rate of zones was constant at 30°C/min. Continuous nitrogen feed (20 ml/min) was applied to maintain an inert atmosphere for the reactions. In order to improve the efficiency of gasification, "*in-situ*" steam generation was used via water injection into the second reaction zone (5 g/h). Gaseous products obtained from the experiments were collected in a Tedlar bag for further analysis. After the reactions took place (approximately 30 min) and the reactor cooled down, solid residue and catalyst were removed from the reactor manually.

2.3. Analysis. Thermogravimetric analysis (TGA) was performed in order to get preliminary information on pyrolysis behavior and to carry out the proximate analysis of the MSW feedstocks. During the analysis, TG 209 F1 Libra equipment was used, with a 35–900°C temperature range (heating rate: 25°C/min). The TGA was conducted in constant nitrogen flow (20 ml/min), to maintain an inert atmosphere.

Analysis of the gaseous product was carried out with a DANI-type gas chromatograph equipped with flame ionization and thermal conductivity detectors. Rtx-1 PONA (100 m × 0.25 mm × 0.5 μm) and Carboxen TM 1006 PLOT (30 m × 0.53 mm) were used as columns. Rtx-1 PONA has been operated with the isothermal condition at 35°C while the injector and detector were at 210°C temperature. In the case of Carboxen TM 1006 PLOT, the following temperature program was applied: 35°C for 18 min, heating with 15°C/min to 120°C, and held at 120°C for 2 minutes. The retention time of components was determined previously with gas standards.

Ni and Ce contentss of catalysts were determined via energy-dispersive X-ray fluorescence analysis (EDX-RF; Shimadzu EDX-8100).

The lower heating value of obtained gases was calculated from the GC results according to the following equation [34].

$$\mathrm{LHV}\left(\frac{\mathrm{MJ}}{\mathrm{Nm}^3}\right) = \frac{(\mathrm{CO}\times 126.36 + \mathrm{H_2}\times 107.98 + \mathrm{CH_4}\times 358.18 + \mathrm{C_2H_2}\times 56.002 + \mathrm{C_2H_4}\times 59.036 + \mathrm{C_2H_6}\times 63.772)}{1000}. \quad (1)$$

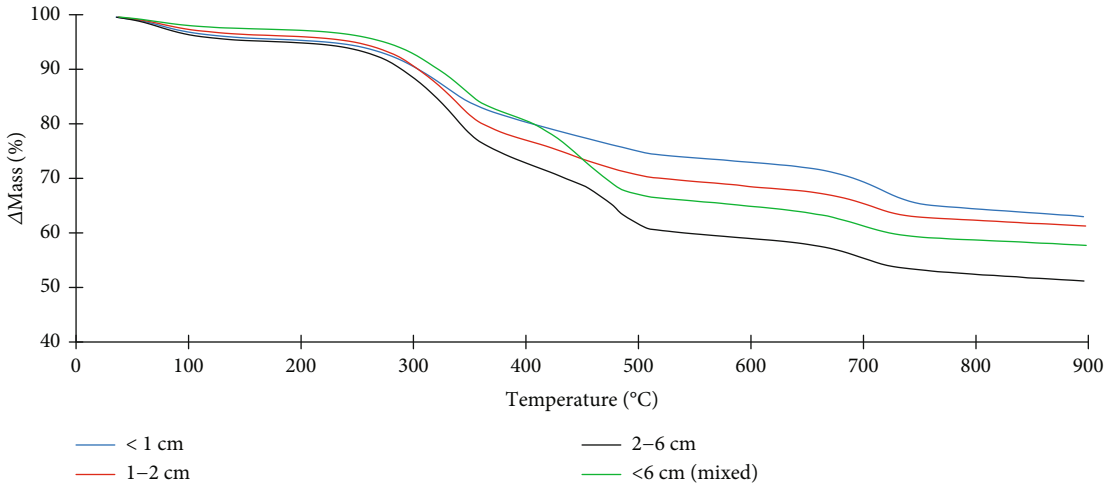

Figure 2: Mass change of the different feedstocks in function of temperature.

Elemental analysis of feedstocks and solid residues obtained from combined pyrolysis and gasification was performed by the Carlo Erba type CHNS/O analyzer. During the analysis, weight percentages of carbon, hydrogen, nitrogen, and sulfur were determined while oxygen + other element content was calculated from the difference.

The gross heating value of solid residues was determined via an automatic oxygen bomb calorimeter (Parr 6200 Calorimeter).

3. Results and Discussion

3.1. Thermal Decomposition Behavior (TGA Analysis). Based on the results of the thermogravimetric analysis, it can be concluded that, in accordance with expectations, the highest residue—accounting for 56.2%—was formed from "soil-like" material with a particle size below 1 cm. In the case of 1-2 cm particle-sized paper-rich material, the residue constituted 45.8%, while the fraction rich in both paper and plastic (2-6 cm) formed residue with 30.4% yield. The residue from the mixed fraction was 28.1%. Curves from the thermogravimetric analysis are illustrated in Figure 2.

The DTG curves (Figure 3) can be obtained by deriving the TG curves, which allow the determination of the decomposition intensities of the feedstock fractions in various temperature ranges. On the DTG curves, four major intensity peaks are predominantly observed. The first peak, within the range of 35-150°C, is attributed to moisture evaporation. Peaks detected between 200 and 650°C are associated with mass reductions caused by the thermal degradation of volatile components. Within this temperature range, the decomposition of easily degradable organic molecules, plastics, cellulose, hemicellulose, and lignin takes place. The presence of the latter is due to the organic content, paper, and textile components of the MSW. The intensity of the first peak (200-400°C) is contributed by the degradation of cellulose and hemicellulose, while the appearance of the second peak is attributed to the degradation of plastics [35]. Above 650°C, the decomposition extends to calcium carbonate and other minerals derived from paper manufacturing or other components of MSW, such as talc, along with the degradation of other inorganic additives, persisting until 800°C [36].

The soil-like fraction (<1 cm) had the lowest content in volatile components, which can be seen in the intensity of the second and third main degradation ranges. Simultaneously, in this case, the most significant fourth degradation range was observed, caused by the inorganic material richness of the feedstock. An intense peak is observed in the third range for the 2-6 cm and for the mixed (<6 cm) fractions, which is attributed to the presence of paper, plastic, and textile content in these fractions.

3.2. Product Yield. Product yields were calculated based on the weight balance based on the following equations:

$$\text{Residue}\,(\%) = \left(\frac{\text{Mass of feedstock}\,(\text{g}) - \text{mass of residue}\,(\text{g})}{\text{Mass of feedstock}\,(\text{g})}\right) * 100,$$
$$\text{Gas product yield}\,(\%) = 100 - \text{residue}\,(\%). \quad (2)$$

During the combined pyrolysis and gasification experiments, no detectable amount of liquid product was formed which was attributed to the small amount of inlet matter as well as to the design and orientation of the tubular kiln reactor. Naturally, as the feedstock contains biomass and plastics, the formation of long-chain hydrocarbons and other oxygenates (aldehydes and ketones) is inevitable. With a sufficient amount of feedstock, the heavy product is a two-phased liquid (organic and aqueous phases), from which, after settling, the quantity of the oily phase can be determined. However, the formation of such a two-phase liquid product was not observed. Due to the horizontal arrangement, the residence time of pyrolysis products in the reactor is longer, resulting in a higher degree of cracking. The presence of biomass also leads to the formation of water, but the quantity of generated water is immeasurable since gasification occurred alongside with water feed (in situ steam generation). Therefore, it is impossible to determine whether the few drops of water present in the mist eliminator originated

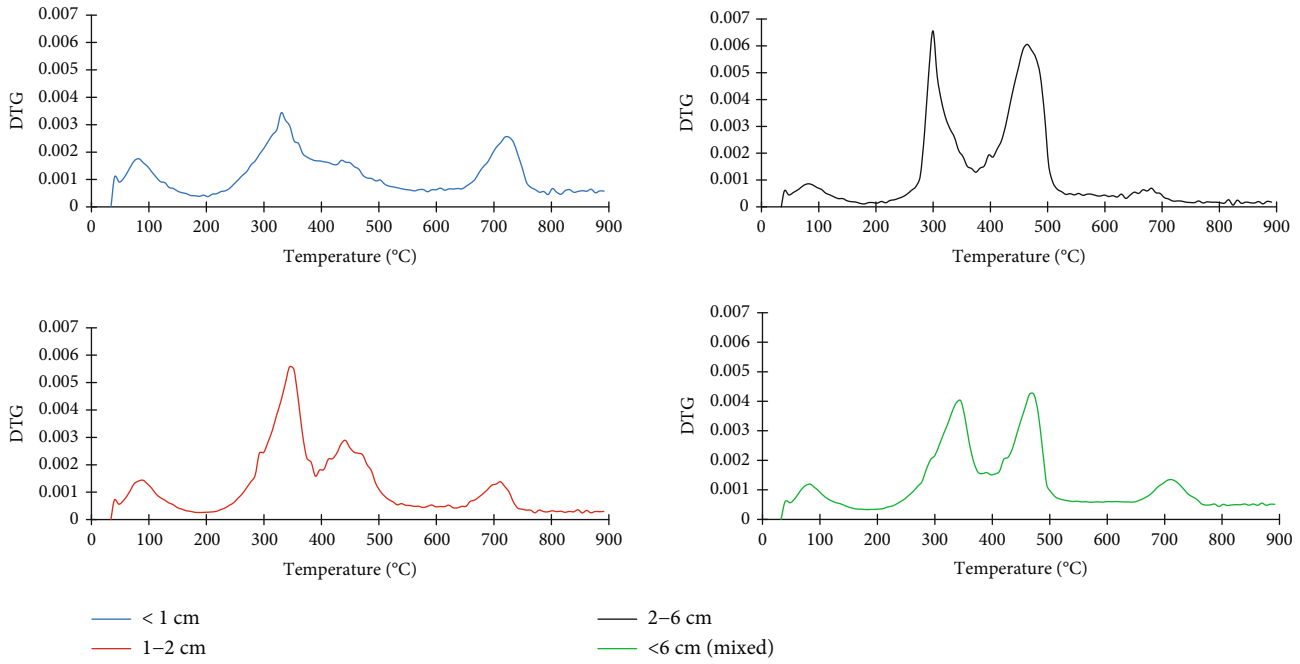

Figure 3: Intensity of mass change in function of temperature (DTG curves).

from unspent steam or were formed during gasification. For these reasons, liquid products were excluded from the yield determination.

Gas product and solid residue yields of the different experiments can be seen in Figure 4. From <1 cm feedstock, 71.3-82.3% solid residue was formed, while the paper and plastic-rich wastes (1-2 cm, 2-6 cm) resulted in the formation of 32.1-57.0% (1-2 cm) and 51.7-61.4% (2-6 cm) of gas products. This tendency is due to the decomposition of paper and plastics in less severe conditions ($T = 500^{\circ}C$) [37] compared to the <1 cm fine material which contained mainly woody biomass and inert components (sand and clay). Temperature rise and the application of catalysts in the second reactor zone had no significant effect on the product yields, because of the fact that the feedstock itself has not been in contact with the catalysts and the higher temperature of the second zone.

3.3. Gas Product Composition. Gas products of thermal and thermocatalytic experiments contained different proportions of hydrogen, carbon monoxide, carbon dioxide, methane, and C_2-C_5 hydrocarbons (Figure 5). The hydrogen and methane content of each product has been increased when the temperature in the second zone was elevated to 900°C, although the carbon-monoxide content decreased in general. Examining the results of several researchers, it can be generally concluded that during gasification, the increasing temperature tends to elevate the CO content while reducing the CH_4 content [38–41]. One possible explanation for this phenomenon could be the thermodynamic favorability of methane steam reforming and the Boudouard reaction (Table 3) at high temperatures, because of the fact that these are highly exothermic reactions. However, in the present case, an opposite trend was observed. One reason for the increase in CO content might be that, due to the CO generated in the Boudouard and other reforming reactions, along with the excess water present, the water-gas shift (WGS) reaction shifted towards product formation even at higher temperatures, given the abundant reactants available. This is consistent with the observed increase in the hydrogen concentration as well. Methane could be formed through the methanization reaction, in which Ni-containing catalysts exhibit high activity [42]. Additionally, the cracking of longer-chained hydrocarbons significantly contributes to methane formation, which occurs more extensively at higher temperatures. Similar conclusions were drawn by Lin et al. [43].

The application of catalysts had an effect on the product composition as well. Products from thermocatalytic combined pyrolysis and gasification contained more hydrogen than those obtained in catalyst-free pyrolysis-gasification, except gas product from <1 cm feedstock. Among the studied catalysts, Ce-impregnated Ni/Y-zeolite seemed to be more advantageous because its application resulted in higher hydrogen content at a lower temperature: 1.5-17.5% more hydrogen content was observed at 600°C from feedstocks with the same composition. In contrast, when the temperature of the 2nd reactor zone was 900°C, no significant difference was observed between the two catalysts. Products obtained from paper and plastic-rich feedstocks (1-2 cm, 2-6 cm) in the presence of Ni-Ce/Y-zeolite contained less CO in lower temperature compared to the combined pyrolysis and gasification over Ni/Y-zeolite.

For hydrogen production, elevated temperature, paper-rich 1-2 cm feedstock, and Ni-Ce/Y-zeolite were the most advantageous (27.7% H_2 content), while lower temperature, organic-rich, <1 cm feedstock, and catalyst-free pyrolysis-gasification favored for the high CO content (64.1%).

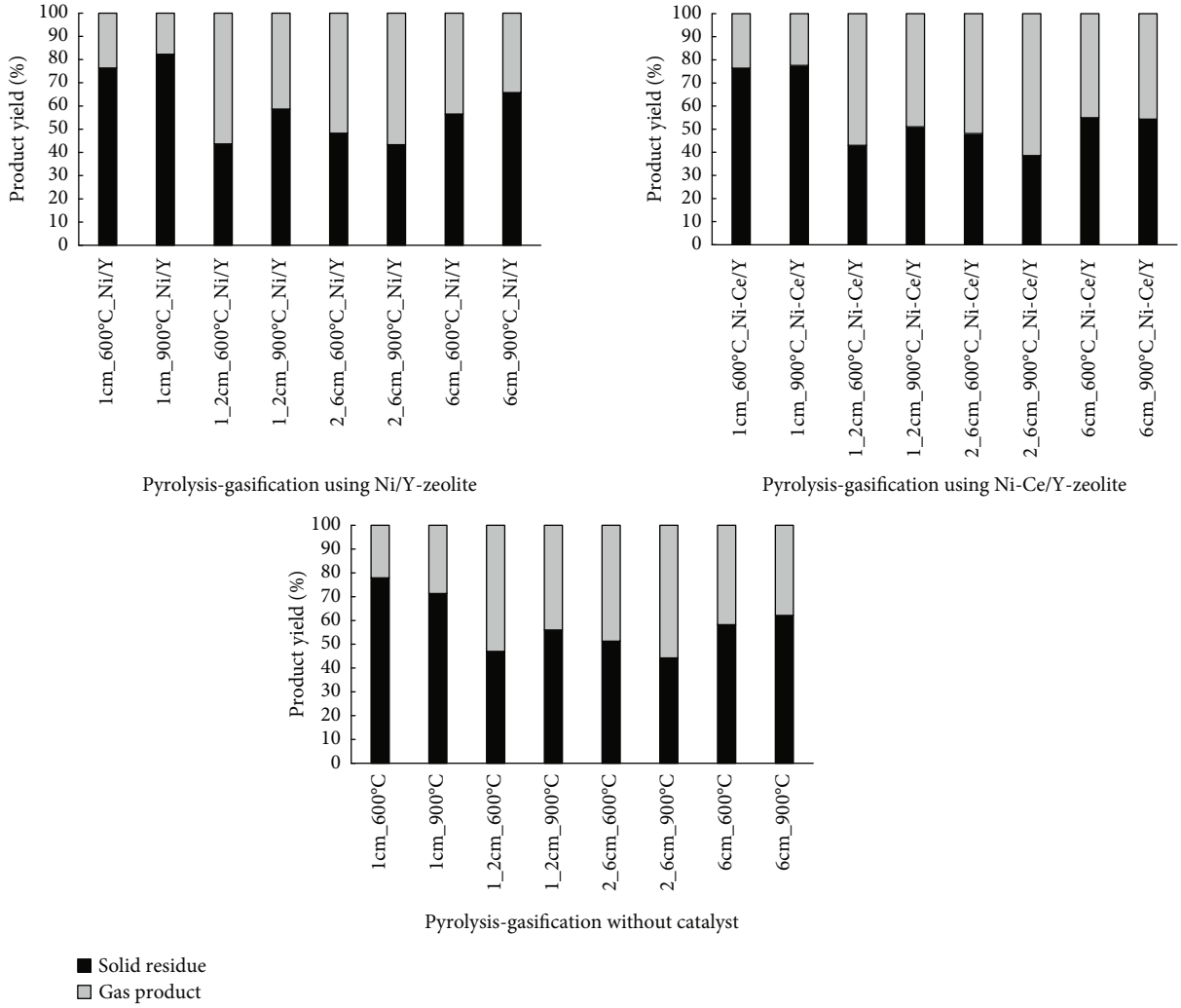

Figure 4: Product yields of combined pyrolysis-gasification experiments.

Methane and C_2-C_5 hydrocarbon formation was observed with the greater extent in the case of paper and plastic-rich 2-6 cm feedstock material, which is contributed to the decomposition of plastic, while products from plastic/paper-rich feedstock (1-2 cm) had the highest CO_2 content at a lower temperature.

During combined pyrolysis and gasification, several consecutive and parallel reactions take place (Table 3). These reactions are endothermic pyrolysis, cracking and reforming reactions, exothermic methanation, and water-gas shift reaction. Different component ratios of gaseous products (H_2/CO, CO_2/CO, and CH_4/CO) can indicate indirectly the occurred reactions.

Different gas component ratios can be seen in Figure 6. For synthetic fuel production, the H_2/CO ratio of the obtained gas product is crucial. Depending on the temperature and the applied catalyst, different H_2/CO of the feed gas is required: for Fischer-Tropsch synthesis where the catalyst has no activity for WGS reaction (e.g., cobalt-based low temperature Fischer-Tropsch), the feed gas should have H_2/CO ratio ≅2.0-2.2, while for Fe-catalyzed Fischer-Tropsch synthesis, relatively low H_2/CO is required (0.5-1.4) [37]. Gaseous products obtained at higher temperatures had significantly higher H_2/CO ratios than those which were formed at 600°C. These tendencies are attributed to a greater extent of endothermic pyrolysis/cracking reactions at higher temperatures. Hydrocarbon and methane steam reforming also could contributed to the high H_2/CO ratios; for example, according to the methane steam reforming reaction, 3 mol hydrogen and 1 mol CO are produced from one mol of methane and water. The usage of Ni-impregnated catalysts also increased the hydrogen to carbon-monoxide ratio. It is important to mention that adding cerium to the Ni/Y-zeolite had a positive effect on the H_2/CO ratio in the case of paper and plastic/paper-rich feedstocks (1-2 cm, 2-6 cm) at the lower temperature, resulting in 0.4-0.45 higher values at 600°C. The highest H_2 to CO ratio was achieved with 2-6 cm feedstock at the higher 2nd zone temperature on nickel/Y-zeolite (H_2/CO: 0.95). The Ni-Ce/Y-zeolite also reduced the H_2/CO difference between the sieved feedstocks and the original mixed <6 cm material. Several factors can influence the CO_2/CO and CH_4/CO ratios of the obtained gas product. Endothermic Boudouard, reverse WGS, and dry and steam reforming reactions decrease the CO_2/CO

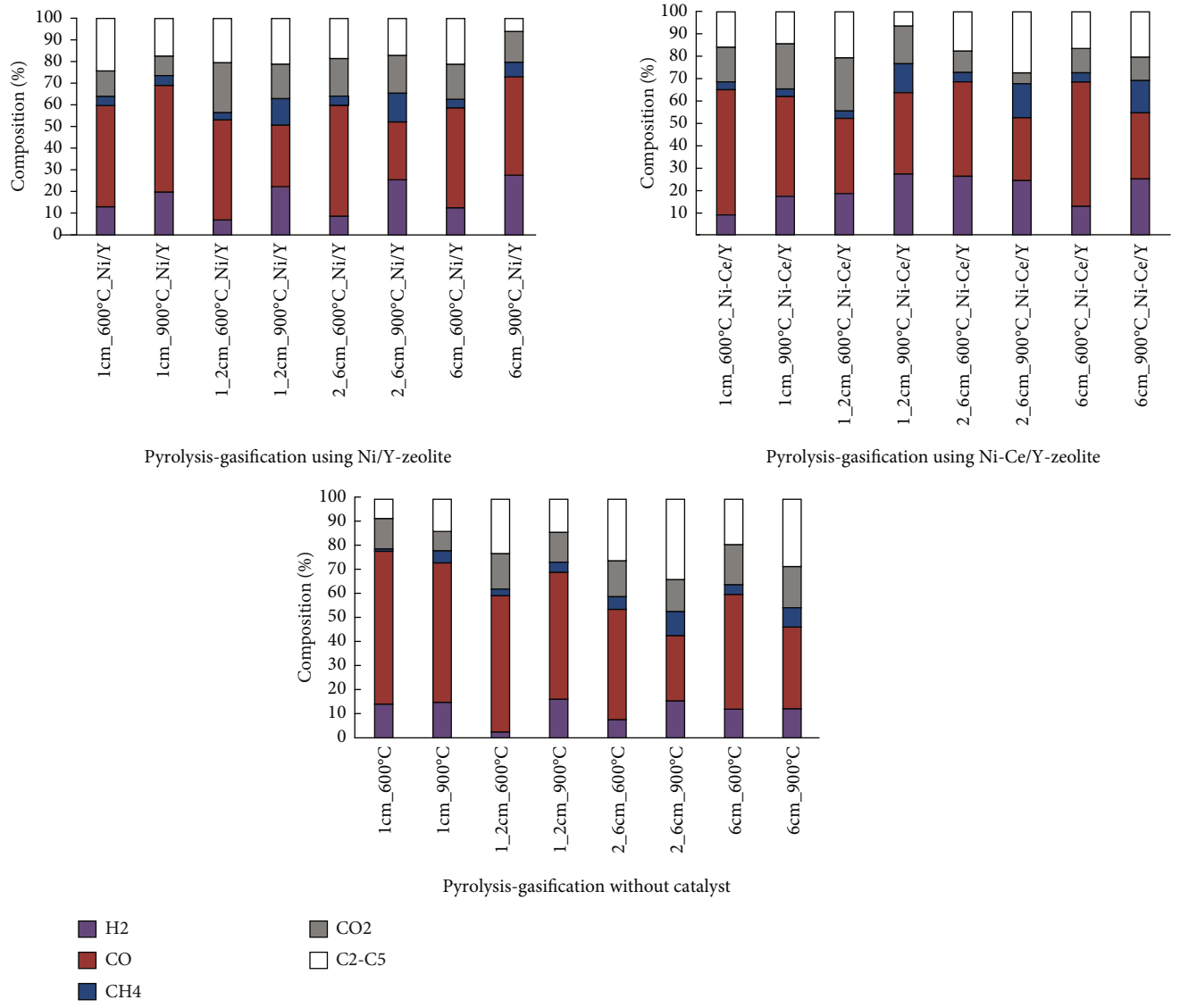

Figure 5: Composition of the obtained gas products.

Table 3: General reactions of pyrolysis-gasification [36].

Name	Reaction equations	ΔH (kJ/mol)
Pyrolysis	Feedstock (e.g.,biomass) $\longrightarrow H_2 + CH_4 + CO + CO_2 + H_2O$ + tar + solid residue	>0
Tar cracking	Tar $\longrightarrow H_2 + CH_4 + CO + CO_2 + H_2O + C_xH_y + C_mH_nO_p$	>0
Catalytic cracking	$C_xH_y \longrightarrow C_{x-m}H_{y-n} + H_2 + CH_4 + \cdots.$	>0
Methane steam reforming	$CH_4 + H_2O \leftrightarrows CO + 3H_2$	206,2
Hydrocarbon steam reforming	$C_xH_y + xH_2O \leftrightarrows xCO + (x + y/2)H_2$	>0
Dry reforming	$C_xH_y + xCO_2 \longrightarrow \frac{2xCO + y}{2H_2}$	>0
Water-gas shift reaction (WGS)	$CO + H_2O \leftrightarrows CO_2 + H_2$	-41,2
Boudouard reaction	$C + CO_2 \leftrightarrows 2CO$	172,5
Methanation reaction	$C + 2H_2 \leftrightarrows CH_4$	-74,9

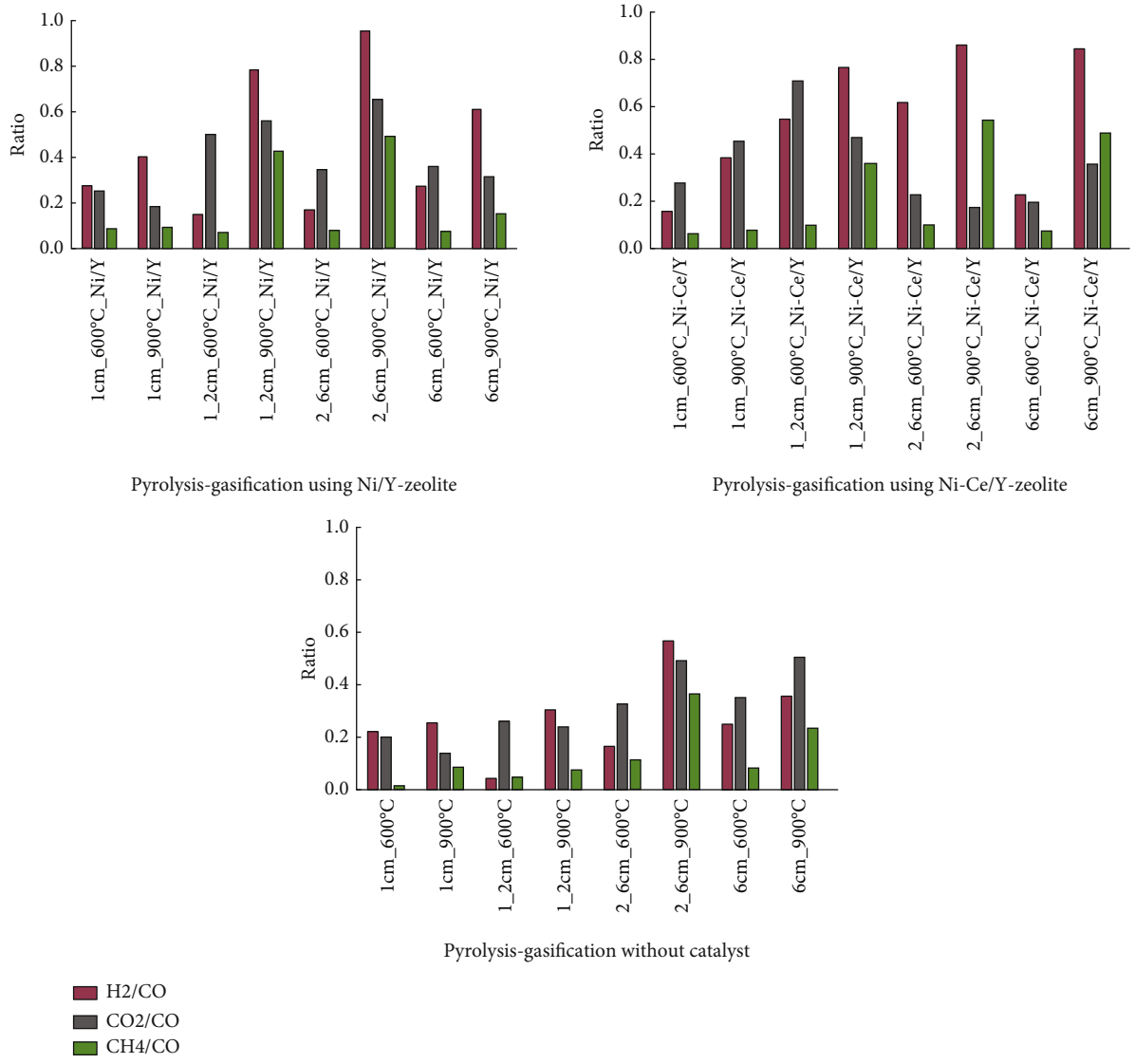

Figure 6: Different component ratios of the obtained gas products.

and CH_4/CO ratios of the obtained gas product in higher temperatures, although the intensification of pyrolysis/cracking reaction, the formed carbon monoxide, and the presence of steam can shift the balance of the equilibrium reactions, resulting in a decrease of these ratios.

3.4. Lower Heating Value of Gas Products. According to equation (1), the methane content of the obtained gas products determined the LHV with the greatest extent followed by the CO and hydrogen content. Hydrocarbon content had little impact compared to other components, while the CO_2 content decreased the LHV. Figure 7 shows the lower heating value of the obtained gas products. The LHV of the gas products varied between 8.7 and 12.6 MJ/Nm^3. As it was mentioned before, the application of 900°C in the second reactor zone resulted in more hydrogen and methane formation; therefore, the LHVs of these products were higher than those which were formed at 600°C (except the <1 cm feedstock with Ni-Ce/Y-zeolite). In the case of catalyst-free experiments, these differences were decreased. Gases obtained from the combined pyrolysis and gasification of 1-2 cm and 2-6 cm feedstock in the presence of Ni-Ce/Y-zeolite had the highest LHVs due to the aforementioned reasons.

3.5. Elemental Composition of Solid Residues (CHNS/O). Based on the CHNS/O results (Figure 8), it was found that the carbon, nitrogen, and hydrogen (and sulfur) content of feedstocks significantly decreased due to the combined pyrolysis and gasification. Significant carbon and hydrogen release could be observed from 1-2 cm and 2-6 cm feedstocks, which may be attributed to the decomposition of high carbon and hydrogen containing plastic and paper. It is important to note that these feedstocks yielded a gas product with a higher yield. No significant differences were found in the function of the temperature of the 2nd zone and the utilization of catalyst, because the feedstock itself was placed to the 1st which was held at 500°C in each experiment; therefore, the results are presented via one experimental setup.

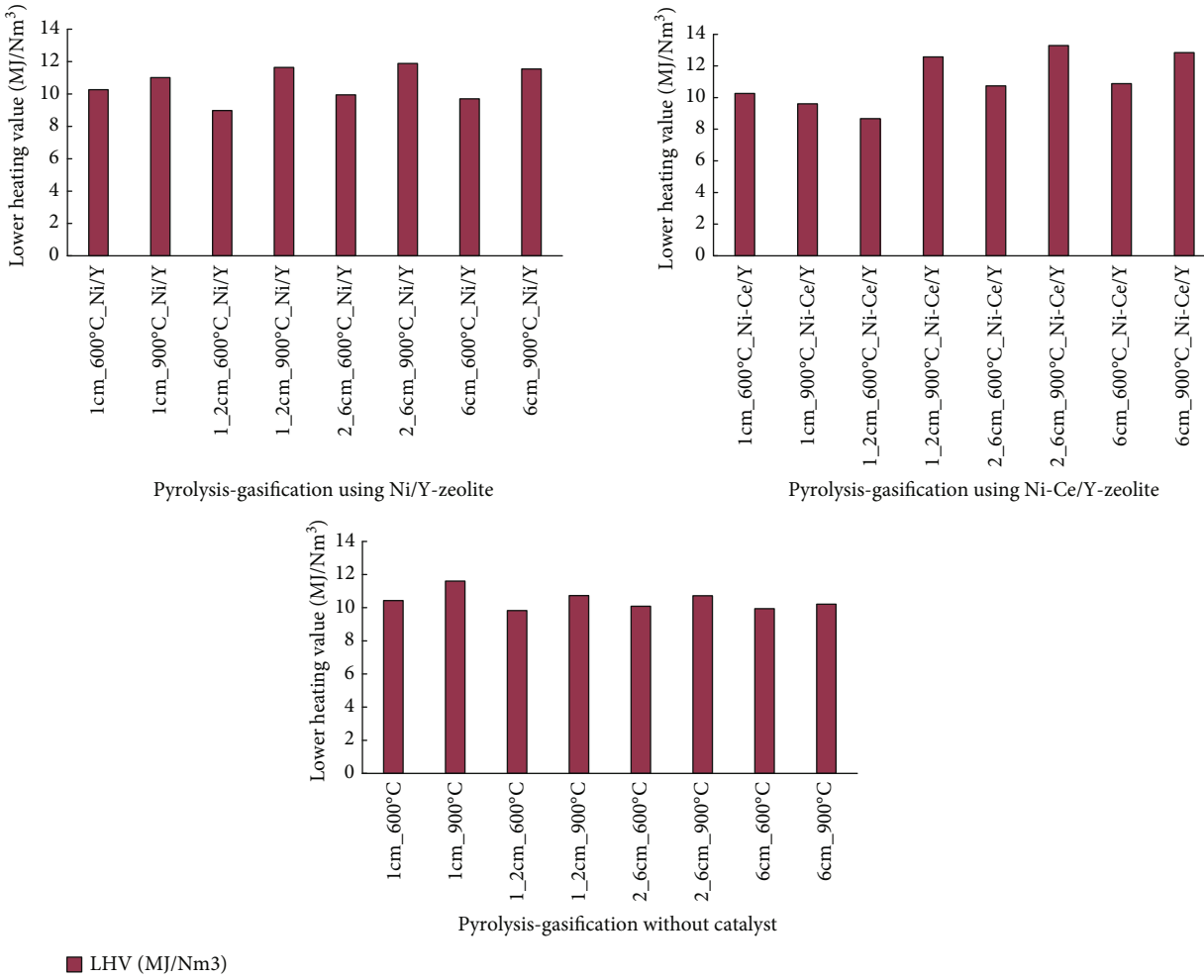

Figure 7: Lower heating values of the obtained gas products.

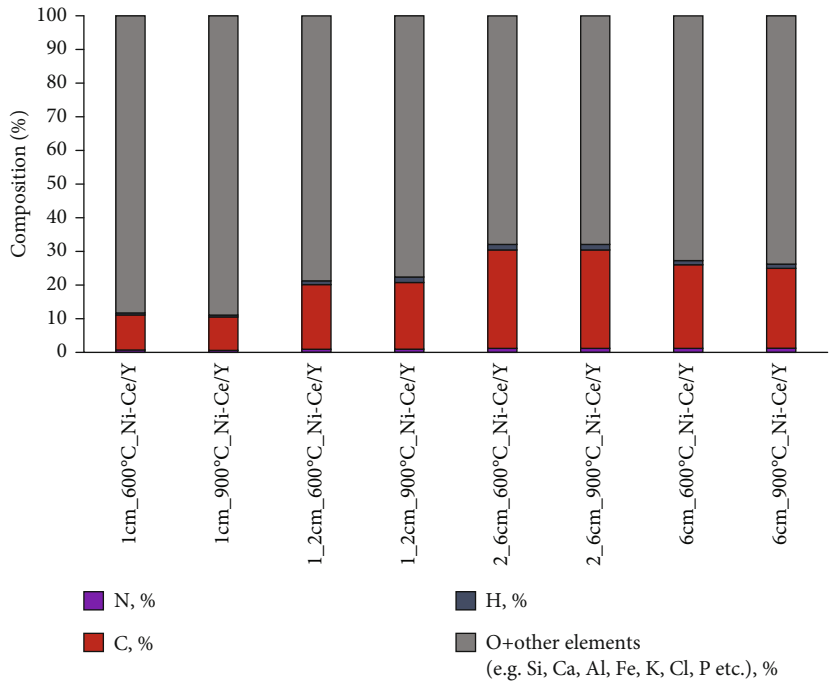

Figure 8: Elemental composition of solid residues on a dry basis (CHNS/(O + other elements)).

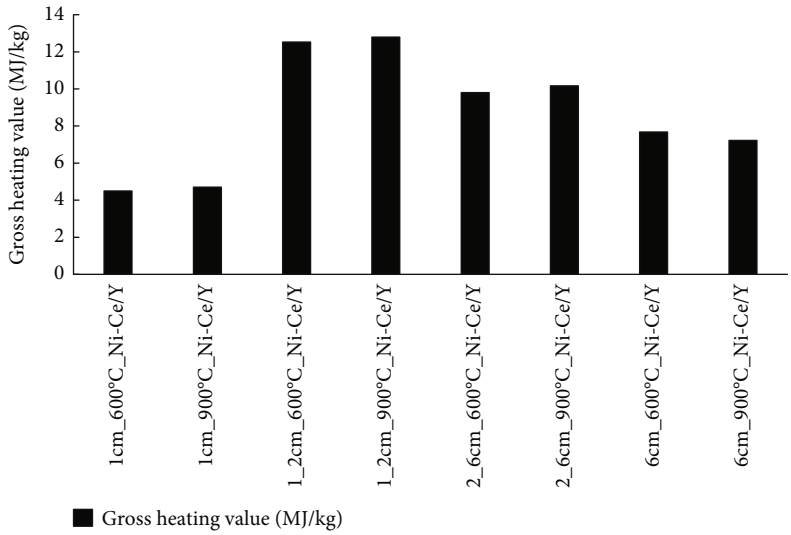

Figure 9: Gross heating values of the solid residues achieved in the presence of Ni-Ce/Y catalyst.

From Figure 6, it can be seen that the related solid residue of <1 cm feedstock, which is low in carbon and hydrogen in general, had the lowest hydrogen and carbon and the highest O+ other element content. This tendency is contributed to the biomass decomposition caused by carbon release and presumably to the high inert material content of this feedstock. Solid residues obtained from the combined pyrolysis and gasification with 1-2 cm feedstock had the highest H/C ratio, which affects the HHV of solid residues.

3.6. Gross Heating Value of Solid Residues. The gross heating value of solid residues has a strong relationship with the elemental composition. The gross heating value increases when the carbon content is lower but also rises with higher hydrogen content [38]. Absolute hydrogen and carbon content as well as hydrogen to carbon ratio can affect the HHV of solid residues. The gross heating values of the obtained solid residues from Ni-Ce/Y-zeolite-promoted pyrolysis-gasification experiments can be seen in Figure 9.

Based on the results, it was found that residues from 1 to 2 cm feedstocks had the highest heating value: 12.5-12.8 MJ/kg. This is consistent with the high hydrogen content and H/C ratio of these residues. Low hydrogen-containing residues from pyrolysis-gasification of <1 cm feedstocks had the lowest gross heating values.

4. Conclusion

In this study, pyrolysis-gasification of various particle-sized OFMSW was investigated at different temperatures in the presence of Ni/Y- and Ni-Ce/Y-zeolites. Product yield, composition, and heating value were determined in the function of feedstock composition, temperature, and catalyst. It was found that usage of 1-2 cm paper and 2-6 cm paper and plastic-rich feedstocks enhanced the yield, hydrogen content, and H_2/CO ratio of the produced gases and, also, the heating value of the solid residue; therefore, these products are the most suitable for Fischer-Tropsch purpose syngas production. In contrast, combined pyrolysis and gasification of <1 cm feedstock yielded the less gas product, with low hydrogen, and high CO content, therefore with the smallest H_2/CO ratio. The application of catalysts in the 2nd zone had a significant effect on gaseous product composition. The highest H_2/CO ratio was observed in the case of paper and plastic-rich 2-6 cm feedstock when Ni/Y-zeolite was used and the 2nd zone at elevated temperature. It was concluded that adding Ce to the nickel/Y-zeolite increased the H_2/CO ratio at lower temperatures, which decreases the energy demand of the whole process. Differences among H_2/CO ratios decreased when Ni-Ce/Y-zeolite was placed in the 2nd zone at 900°C, which gives the conclusion that in this catalyst and temperature combination, the mixed feedstock (<6 cm) can be used sufficiently; therefore, separation of the OFMSW is not necessary. Although at 600°C temperature, 1-2 cm or especially the 2-6 cm feedstock and the application of Ni-Ce/Y-zeolite are recommended due to the significantly higher H_2/CO ratio of the obtained gas products. It can be also concluded that <1 cm feedstock cannot be used sufficiently in the examined pyrolysis-gasification system separately. It can be concluded that except for the fine fraction (<1 cm), pyrolysis/gasification is a promising technical option for energy recovery from OFMSW.

Abbreviations

AD: Anaerobic digestion
Ce: Cerium
MBT: Mechanical-biological treatment
MSW: Municipal solid waste
Ni: Nickel
OFMSW: Organic fraction of municipal solid waste
RDF: Refuse derived fuel.

Data Availability

The data that support the findings of this study are available from the corresponding author upon reasonable request.

Conflicts of Interest

The authors declare that there are no conflicts of interest regarding the publication of this article.

Acknowledgments

This work has been implemented by the TKP2021-NKTA-21 project with the support provided by the Ministry for Innovation and Technology of Hungary from the National Research, Development and Innovation Fund, financed under the 2021 Thematic Excellence Programme funding scheme.

References

[1] "BP Statistical Review of World Energy – 71st edition, BP," 2022, https://www.bp.com/en/global/corporate/energy-economics/statistical-review-of-world-energy.html.

[2] "IEA World Energy Investment 2022, IEA, Paris 2022," https://www.iea.org/reports/world-energy-investment-2022.

[3] S. Kaza, L. Yao, P. Bhada-Tata, and F. Van Woerden, *What a waste – a global snapshot of solid waste management to 2050, Urban Development*, World Bank, Washington DC, 2018, https://openknowledge.worldbank.org/handle/10986/30317.

[4] "EuroStat Municipal Waste Statistic," 2021. https://ec.europa.eu/eurostat/statistics-explained/index.php?title=Municipal_waste_statistics#Municipal_waste_generation.

[5] M. D. Vaverkova, "Landfill impacts on the environment—review," *Geosciences*, vol. 9, no. 10, p. 431, 2019.

[6] M. C. Di Lonardo, F. Lombardi, and R. Gavasci, "Characterization of MBT plants input and outputs: a review," *Reviews in Environmental Science and Bio/Technology*, vol. 11, no. 4, pp. 353–363, 2012.

[7] M. Malinowski, "Biostabilization process of undersized fraction of municipal solid waste with biochar addition," *Journal of Material Cycles and Waste Management*, vol. 24, no. 6, pp. 2201–2215, 2022.

[8] The Council of the European Union, "Council Directive 1999/31/EC of 26 April 1999 on the landfill of waste, Official Journal L, 1999, 182, 0001 – 0019," https://eur-lex.europa.eu/legal-content/EN/TXT/HTML/?uri=CELEX:31999L0031%26from=EN.

[9] The European Parliament and the Council of the European Union, "Directive (EU) 2018/850 of the European Parliament and of the Council amending Directive 1999/31/EC on the landfill of waste," *Official Journal L*, vol. 150, pp. 100–108, 2018, https://eur-lex.europa.eu/legal-content/EN/TXT/HTML/?uri=CELEX:32018L0850%26from=HU.

[10] S. Nanda and F. Berruti, "Municipal solid waste management and landfilling technologies: a review," *Environmental Chemistry Letters*, vol. 19, no. 2, pp. 1433–1456, 2021.

[11] R. Babu, P. M. Prieto Veramendi, and E. R. Rene, "Strategies for resource recovery from the organic fraction of municipal solid waste," *Case Studies in Chemical and Environmental Engineering*, vol. 3, article 100098, 2021.

[12] R. Campuzano and S. González-Martínez, "Characteristics of the organic fraction of municipal solid waste and methane production: a review," *Waste Management*, vol. 54, pp. 3–12, 2016.

[13] E. M. Barampouti, S. Mai, D. Malamis, K. Moustakas, and M. Loizidou, "Liquid biofuels from the organic fraction of municipal solid waste: a review," *Renewable and Sustainable Energy Reviews*, vol. 110, pp. 298–314, 2019.

[14] M. Lucian, M. Volpe, F. Merzari et al., "Hydrothermal carbonization coupled with anaerobic digestion for the valorization of the organic fraction of municipal solid waste," *Bioresource Technology*, vol. 314, article 123734, 2020.

[15] F. Núñez, M. Pérez, L. F. Leon-Fernández, J. L. García-Morales, and F. J. Fernández-Morales, "Effect of the mixing ratio on the composting of OFMSW digestate: assessment of compost quality," *Journal of Material Cycles and Waste Management*, vol. 24, no. 5, pp. 1818–1831, 2022.

[16] V. Esmaeili, J. Ajalli, A. Faramarzi, M. Abdi, and M. Gholizadeh, "Gasification of wastes: the impact of the feedstock type and co-gasification on the formation of volatiles and char," *International Journal of Energy Research*, vol. 44, no. 5, pp. 3587–3606, 2020.

[17] C. J. Roos, *Clean heat and power using biomass gasification for industrial and agricultural projects*, U.S. Department of Energy–Clean Energy Application Center, 2010.

[18] D. M. del Monte, A. J. Vizcaíno, J. Dufour, and C. Martos, "Potential pathways for syngas transformation towards kerosene range hydrocarbons in a dual Fischer-Tropsch-zeolitebed," *International Journal of Energy Research*, vol. 46, no. 4, pp. 5280–5287, 2022.

[19] S. M. Islam, M. Y. Miah, M. Ismail, M. S. Jamal, S. K. Banik, and M. Saha, "Production of bio-oil from municipal solid waste by pyrolysis," *Bangladesh Journal of Scientific and Industrial Research*, vol. 45, no. 2, pp. 91–94, 2010.

[20] I. Firtina-Ertis, N. Ayvaz-Cavdaroglu, and A. Coban, "An optimization-based analysis of waste to energy options for different income level countries," *International Journal of Energy Research*, vol. 45, no. 7, pp. 10794–10807, 2021.

[21] N. B. Klinghoffer and M. J. Castaldi, *Gasification and pyrolysis of municipal solid waste (MSW)*, Woodhead Publishing Series in Energy, 2013.

[22] S. Mariyam, M. Shahbaz, T. Al-Ansari, H. R. Mackey, and G. Mckay, "A critical review on co-gasification and co-pyrolysis for gas production," *Renewable and Sustainable Energy Reviews*, vol. 161, article 112349, 2022.

[23] M. M. Hasan, M. G. Rasul, M. M. K. Khan, N. Ashwath, and M. I. Jahirul, "Energy recovery from municipal solid waste using pyrolysis technology: a review on current status and developments," *Renewable and Sustainable Energy Reviews*, vol. 145, article 111073, 2021.

[24] J. S. Lu, Y. Chang, C. S. Poon, and D. J. Lee, "Slow pyrolysis of municipal solid waste (MSW): a review," *Bioresource Technology*, vol. 312, article 123615, 2020.

[25] Q. Li, A. Faramarzi, S. Zhang, Y. Wang, X. Hu, and M. Gholizadeh, "Progress in catalytic pyrolysis of municipal solid waste," *Energy Conversion and Management*, vol. 226, p. 113525, 2020.

[26] M. He, B. Xiao, S. Liu et al., "Syngas production from pyrolysis of municipal solid waste (MSW) with dolomite as downstream catalysts," *Journal of Analytical and Applied Pyrolysis*, vol. 87, no. 2, pp. 181–187, 2010.

[27] R. Nandhini, D. Berslin, B. Sivaprakash, N. Rajamohan, and D. V. N. Vo, "Thermochemical conversion of municipal solid waste into energy and hydrogen: a review," *Environmental Chemistry Letters*, vol. 20, no. 3, pp. 1645–1669, 2022.

[28] J. A. Onwudili, C. Muhammad, and P. T. Williams, "Influence of catalyst bed temperature and properties of zeolite catalysts on pyrolysis-catalysis of a simulated mixed plastics sample for the production of upgraded fuels and chemicals," *Journal of the Energy Institute*, vol. 92, no. 5, pp. 1337–1347, 2019.

[29] X. Li, H. Zhang, J. Li, L. Su, J. Zou, and S. Komarneni, "Improving the aromatic production in catalytic fast pyrolysis of cellulose by co-feeding low-density polyethylene," *Applied Catalysis A: General*, vol. 455, pp. 114–121, 2013.

[30] M. do Carmo Rangel, F. M. Mayer, M. da Silva Carvalho, G. Saboia, and A. M. de Andrade, "Selecting catalysts for pyrolysis of lignocellulosic biomass," *Biomass*, vol. 3, pp. 31–63, 2023.

[31] C. Wu and P. T. Williams, "Pyrolysis–gasification of post-consumer municipal solid plastic waste for hydrogen production," *International Journal of Hydrogen Energy*, vol. 35, no. 3, pp. 949–957, 2010.

[32] D. Yao, H. Yang, H. Chen, and P. T. Williams, "Investigation of nickel-impregnated zeolite catalysts for hydrogen/syngas production from the catalytic reforming of waste polyethylene," *Applied Catalysis. B, Environmental*, vol. 227, pp. 477–487, 2018.

[33] M. Al-asadi and N. Miskolczi, "Hydrogen rich products from waste HDPE/LDPE/PP/PET over Me/Ni-ZSM-5 catalysts combined with dolomite," *Journal of the Energy Institute*, vol. 96, pp. 251–259, 2021.

[34] M. H. Yung, A. K. Starace, M. Calvin, A. M. Crow, C. M. Leshnov, and A. Magrini, "Biomass catalytic pyrolysis on Ni/ZSM-5: effects of nickel pretreatment and loading," *Energy & Fuels*, vol. 30, no. 7, pp. 5259–5268, 2016.

[35] B. Kuspangaliyeva, B. Suleimenova, D. Shah, and Y. Sarbassov, "Thermogravimetric study of refuse derived fuel produced from municipal solid waste of Kazakhstan," *Applied Sciences*, vol. 11, no. 3, p. 1219, 2021.

[36] Z. Y. Lai, X. Q. Ma, Y. T. Tang, and H. Lin, "Thermogravimetric analysis of the thermal decomposition of MSW in N2, CO2 and CO2/N2 atmospheres," *Fuel Processing Technology*, vol. 102, pp. 18–23, 2012.

[37] N. Sophonrat, L. Sandstrom, I. N. Zaini, and W. Yang, "Stepwise pyrolysis of mixed plastics and paper for separation of oxygenated and hydrocarbon condensates," *Applied Energy*, vol. 229, pp. 314–325, 2018.

[38] M. He, Z. Hu, B. Xiao et al., "Hydrogen-rich gas from catalytic steam gasification of municipal solid waste (MSW): influence of catalyst and temperature on yield and product composition," *International Journal of Hydrogen Energy*, vol. 34, no. 1, pp. 195–203, 2009.

[39] U. Lee, J. N. Chung, and H. A. Ingley, "High-temperature steam gasification of municipal solid waste, rubber, plastic and wood," *Energy Fuels*, vol. 28, no. 7, pp. 4573–4587, 2014.

[40] R. H. Zeng, S. Z. Wang, and J. J. Cai, "Study on air gasification characteristics of straw in tube furnace," *IOP Conference Series: Earth and Environmental Science*, vol. 188, article 012049, 2018.

[41] S. W. Han, J. J. Lee, D. Tokmurzin et al., "Gasification characteristics of waste plastics (SRF) in a bubbling fluidized bed: effects of temperature and equivalence ratio," *Energy*, vol. 238, article 121944, 2022.

[42] P. Frontera, A. Macario, M. Ferraro, and P. L. Antonucci, "Supported catalysts for CO2 methanation: a review," *Catalysts*, vol. 7, no. 12, p. 59, 2017.

[43] C. Lin, W. Zuo, S. Yuan, P. Zhao, and H. Zhou, "Effect of moisture on gasification of hydrochar derived from real-MSW," *Biomass and Bioenergy*, vol. 178, article 106976, 2023.